Electronic Structure and Redox Properties of the Open-Shell Metal−Carbide Endofullerene $Sc_3C_2@C_{80}$: A Density Functional Theory Investigation

Kai Tan and Xin Lu*

State Key Laboratory of Physical Chemistry of Soild Surface and Center for Theoretical Chemistry, Department of Chemistry, Xiamen University, Xiamen 361005, China

Received: October 26, 2005; In Final Form: November 21, 2005

Density functional theory calculations have shown that the open-shell metal−carbide endofullerene $Sc_3C_2@C_{80}$ has the valence state $(Sc^{3+})_3(C_2)^{3-}@^{C}{}_{80}{}^{6-}$. A lot of low-lying isomers differing in geometries and locations of the endohedral $[(Sc^{3+})_3(C_2)^{3-}]$ cluster have been located, indicating unusual dual intramolecular dynamic behaviors of this endofullerene at room temperature. The electrochemical redox properties of this endofullerene have been elucidated in terms of electronic structure theory. Its redox states are found to follow the general charge−state formula $(Sc^{3+})_3C_2{}^{(3-q)-}@C_{80}{}^{6-}$ (q is the charge of the whole molecule ranging from +1 to −3), demonstrating the high charge flexibility of the endohedral metal−carbide cluster. The structure of the endohedral $[(Sc^{3+})_3C_2{}^{(3-q)-}]$ cluster varies with the redox processes, shifting from a planar structure (for $q = 0$ and −1) to a trifoliate structure (for $q = +1, -2, -3$).

1. Introduction

Endohedral metallofullerenes are such a unique class of fullerene derivatives that have a metal atom or a metal-containing cluster encased in a hollow carbon cage. An interesting common feature of endofullerenes is their "super-atomic" core (postive)−shell (negative) structures arising from the inherent electron transfer from the encapsulated metal or cluster to the carbon cage.[1] The number of electrons transferred is a key factor that governs the stability of the otherwise unstable fullerene cages,[2] exemplified by those endofullerenes (e.g., $Sc_2@C_{66}$,[2] $Sc_3N@C_{68}$[3], and $La_2@C_{72}$[4]) that have carbon cages violating the well-known isolated pentagon rule (IPR).[5] Because of their fascinating geometric and electronic structures, endofullerenes have attracted intense interests in exploration of their physical and chemical properties and potential applications.[1]

Thus far, a large number of endofullerenes have been synthesized and characterized; the endohedral species disclosed varies from a simple metal atom (e.g., M = Sc, Y, La in $M@C_{82}$[1]), a dimetallic cluster (e.g., La_2 in $La_2@C_m$ (m = 72,80)),[4,6] a trimetal−nitride cluster (e.g., Sc_3N in $Sc_3N@C_n$ (n = 68, 78, 80)),[3,7] to a metal carbide cluster (e.g., Sc_2C_2 in $Sc_2C_2@C_{84}$[8] Ti_2C_2 in $Ti_2C_2@C_{78}$[9] and Sc_3C_2 in $Sc_3C_2@C_{80}$[10]). Among them, the endofullerene $Sc_3C_2@C_{80}$ that has the largest endohedral cluster (Sc_3C_2) encapsulated in an I_h-symmetric C_{80} cage appears to be the most interesting. This endofullerene possessing an open-shell electronic configuration was first synthesized and isolated in 1992.[11] Thereafter, it has been extensively characterized by means of electron-spin resonance (ESR),[11,12] UV−Vis,[12a] cyclic voltammetry (CV),[13] and synchrotron radiation X-ray power diffraction.[14] It has long been thought to have a simple endohedral $Sc_3@C_{82}$ structure.[11−15] Previous density functional theory (DFT) calculations[15b] suggested that the $Sc_3@C_{82}$ structure had a charge state of $(Sc^{2+})_3@C_{82}{}^{6-}$, in which the C_{82} cage can be a C_{3v}-symmetric IPR-satisfying isomer or a C_{2v}-symmetric non-IPR isomer (coded #39705 by following the spiral algorithm[16]). On the contrary, Iiduka et al.[10] reported very recently ^{13}C NMR and X-ray diffraction experiments on the monoanion of Sc_3C_{82} and its derivatives and demonstrated unambiguously the endohedral metal carbide structure $Sc_3C_2@C_{80}$ with a Sc_3C_2 cluster being encased in an I_h-symmetric C_{80} cage. Two structural features of this unique endofullerene should be noted here: (i) the Sc_3C_2 cluster may rotate freely within the carbon cage at room temperature, as was implied by ESR (for neutral molecule) and ^{13}C NMR (for monoanion) experiments; and (ii) the geometry of the encased Sc_3C_2 cluster is somewhat elusive, either in a planar structure or in a trifoliate structure (Chart 1).[10]

CHART 1: Two Possible Geometries of Sc_3C_2 Cluster Encased in C_{80}: (a) Planar and (b) Trifoliate

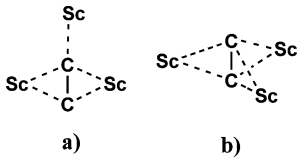

The aim of the present theoretical investigation is multifold: (i) to unravel the electronic structure of $Sc_3C_2@C_{80}$, (ii) to explore the redox properties of $Sc_3C_2@C_{80}$, and (iii) to see how the structure of the encased cluster responds to the redox-charging process.

2. Computational Details

All DFT calculations were performed with the GGA-BLYP functional[17] using the Dmol^3 code.[18] For open-shell systems, the spin-unrestricted algorithm was employed. Double numerical plus polarization (DNP) basis sets without frozen core, which are of the highest quality among all the available basis sets within the Dmol^3 code, were employed for Sc and C atoms. Geometry optimizations were performed with the BFGS algorithm at the GGA-BLYP/DNP level of theory. We have tested another density functional, GGA-P91,[19] which gives results essentially similar to the BLYP predictions (Supporting Infor-

* To whom correspondence should be addressed. E-mail: xinlu@xmu.edu.cn. Tel: +86-592-2181600. Fax: +86-592-2183047.

10.1021/jp056145f CCC: $33.50
Published on Web 01/04/2006

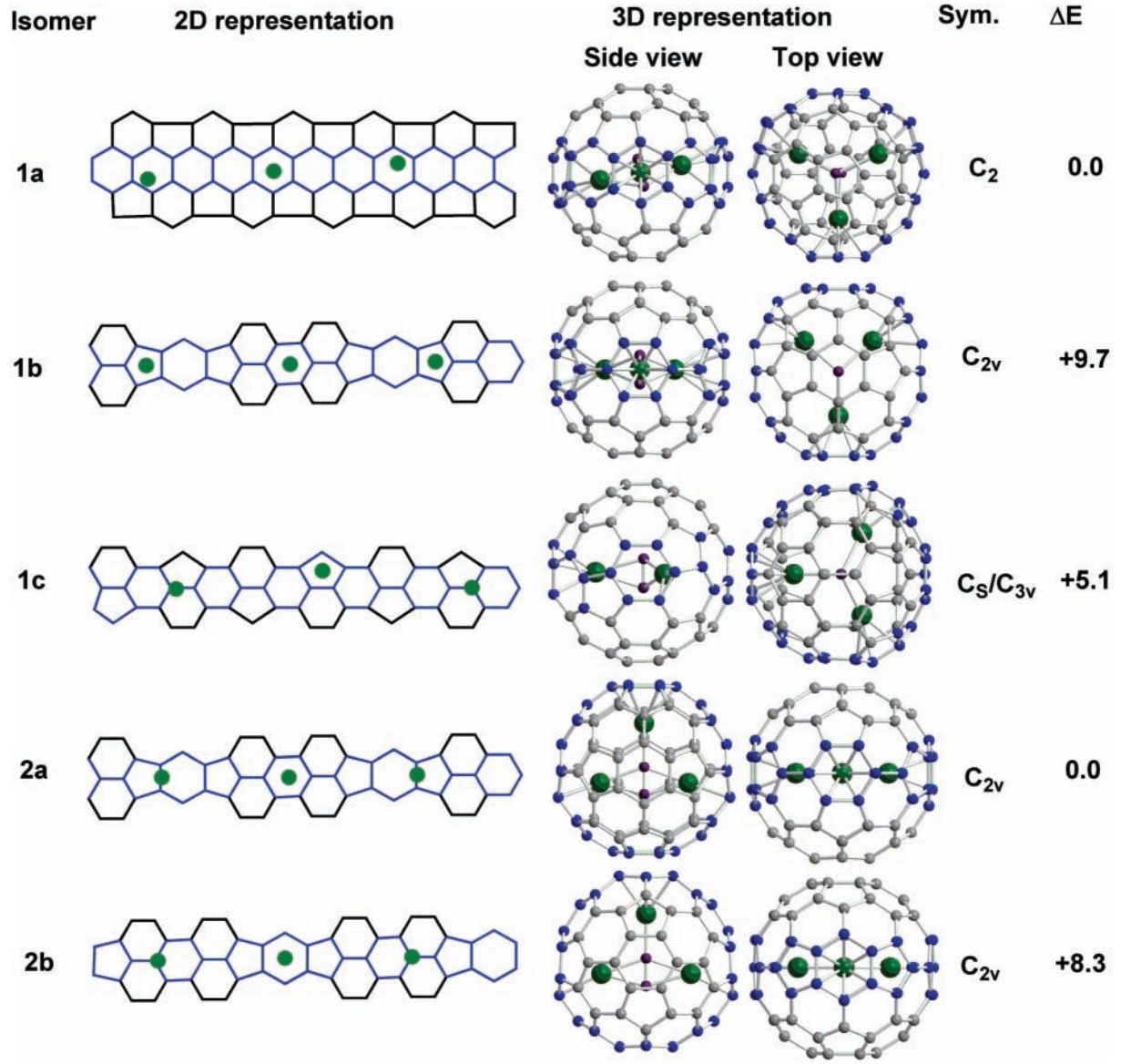

Figure 1. Symmetries, 2D schemes, and 3D ball-stick representations for the GGA-BLYP/DNP-optimized isomers of $Sc_3C_2@C_{80}$ (**1a**−**2b**). The Sc atoms are represented by green dots in the 2D representations. Reported energies (ΔE, in kcal/mol) are relative to $Sc_3C_2@C_{82}$ **1a**.

mation). Since $Sc_3C_2@C_{80}$ has an open-shell doublet electronic configuration, spin contamination of high spin states may be a problem for an accurate description of its doublet ground state with use of the unrestricted Hartree−Fock (UHF) wave functions.[20] However, previous theoretical investigations on a large number of neutral radicals showed that DFT-based "unrestricted Kohn−Sham (UKS) wave function is much less spin contaminated by higher spin states than its UHF counterparts".[21] So we did not consider the spin contamination effect in our DFT calculations.

3. Results and Discussion

3.1. Geometric and Electronic Structures of $Sc_3C_2@C_{80}$ Isomers. We have performed GGA-BLYP/DNP calculations on various possible structures of Sc_3C_2 encapsulated in the C_{80} (I_h) cage. As depicted in Figure 1, five isomers, **1a**−**2b**, have been located as stationary points. For isomers **1a**−**1c**, the trapped Sc_3C_2 cluster is trifoliate with the C−C axis being nearly perpendicular to the Sc_3 plane. The C_2-symmetric isomer **1a** with a ^{2}A electronic state was obtained by aligning the C−C axis of Sc_3C_2 cluster along an S_5 axis of the C_{80} (I_h) cage, but upon geometry optimization the C−C axis tilts away from the S_5 axis in the final geometry. Aligning the C−C axis of Sc_3C_2 cluster along a C_3 axis of the C_{80} (I_h) cage leads eventually to the C_s-symmetric isomer **1c** in a ^{2}A″ electronic state. The C_{2v}-symmetric isomer **1b** has a $^2B_1$ electronic state. Among these three isomers, **1a** is the most stable. However, the energy discrepancies between these isomers are smaller than 10 kcal/mol, suggesting that the trifoliate Sc_3C_2 cluster can readily rotate within the carbon cage at room temperature.

For isomers **2a** (in a $^2B_2$ state) and **2b** (in a $^2B_1$ state), the encased Sc_3C_2 cluster is planar, in sharp contrast to the trifoliate ones in isomers **1a**−**1c**. Both isomers **1a** and **2a** have equally the lowest total energy, implying that the Sc_3C_2 cluster encapsulated in the C_{80} cage may readily fluctuate between the planar structure (in isomer **2a**) and trifoliate structure (in isomer **1a**). This confirms the previous B3LYP prediction reported by Iiduka et al.[10]

Local views of the Sc_3C_2 clusters in isomers **1a** and **2a** are depicted in Figures 2 and 3, respectively. The C−C bond length of the encased Sc_3C_2 cluster is ∼1.31 Å in isomer **1a** (Figure 2) and ∼1.29 Å in isomer **2a** (Figure 3), even shorter than the

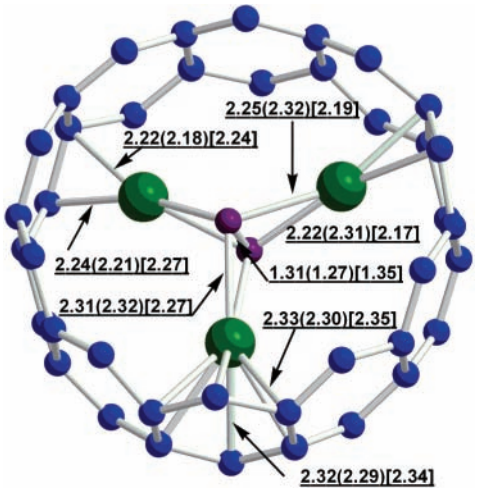

Figure 2. Local view (around the equatorial [10]cyclacene part) of the Sc_3C_2 cluster in $Sc_3C_2@C_{80}$ isomer **1a** and the key atomic distances (Å) for the neutral, cationic (in parentheses), and anionic (in square brackets) forms of $Sc_3C_2@C_{80}$ **1a**.

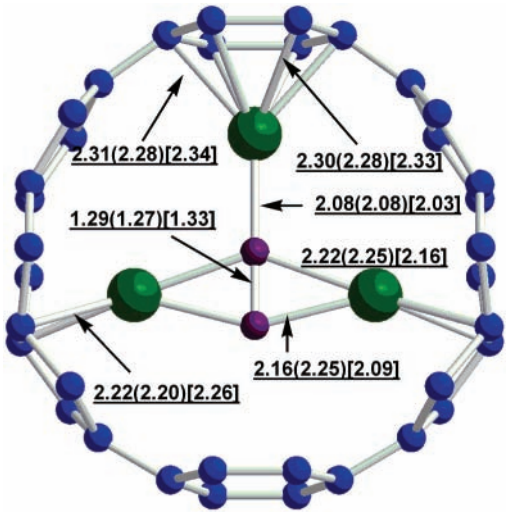

Figure 3. Local view of the Sc_3C_2 cluster in $Sc_3C_2@C_{80}$ isomer **2a** and the key atomic distances (Å) for the neutral, cationic (in parentheses), and anionic (in square brackets) forms of $Sc_3C_2@C_{80}$ **2a**.

lowest limit (~1.32 Å) for tetraanion C_2^{4-} in inorganic compounds.[22,23] So the C_2 moiety should have a charge state lower than −4.

For all five isomers, a careful inspection of their KS wave functions revealed that they are essentially in a valence state of $(Sc_3C_2)^{6+}@C_{80}^{6-}$, in which the spin−unpaired electron is localized within the $(Sc_3C_2)^{6+}$ cluster. For the most stable isomers **1a** and **2a**, their singly occupied molecular orbitals (SOMO) are shown in Figures 4a and 5a, respectively. For each isomer, the SOMO is localized within the encased $(Sc_3C_2)^{6+}$ cluster and is primarily attributed to the covalent dative bonding between the d_π atomic orbitals of Sc^{3+} atoms and the π^* orbital of the C_2 moiety. Hence the C_2 moiety in the encased cluster can be described as C_2^{3-}, and all the Sc atoms are in the formal charge of +3.[24,25] In detail, the valence state of the whole molecule is $(Sc^{3+})_3(C_2)^{3-}@C_{80}^{6-}$. This reminds us of the very stable endofullerene $Sc_3N@C_{80}$ that has analogously a charge state of $(Sc^{3+})N^{3-}@C_{80}^{6-}$.[7a,26] The present DFT prediction, together with the previous work by Iiduka et al., contradicts the previous MEM/Rietveld analysis on Sc_3C_{82}.[14] The MEM/Rietveld analysis suggested a charge state of $(Sc^{+})_3@C_{82}^{3-}$,[14] which is wrong in either structure or charge distribution.

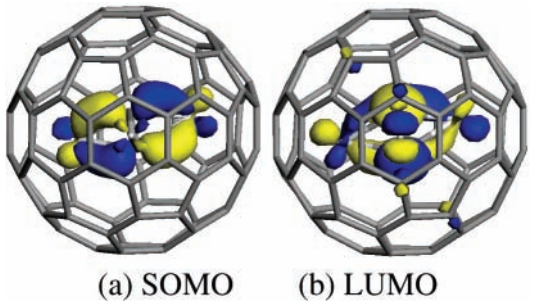

Figure 4. Isodensity surface plots for the (a) SOMO and (b) LUMO of $Sc_3C_2@C_{80}$ isomer **1a**.

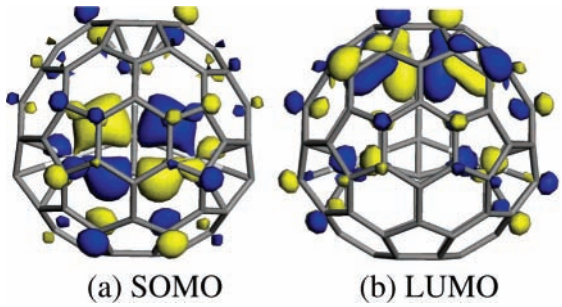

Figure 5. Isodensity surface plots for the (a) SOMO and (b) LUMO of $Sc_3C_2@C_{80}$ isomer **2a**.

Similarly, for $Sc@C_{82}$, the MEM/Rietveld determined charge state is $Sc^{2+}@C_{82}^{2-}$, whereas the recent DFT computation disclosed unambiguously a valence state of $Sc^{3+}@C_{82}^{3-}$.[25] These facts indicate that the MEM/Rietveld analysis of synchrotron X-ray power diffraction data is sometimes unreliable, despite the fact that this technique has been widely accepted for structural determination of endofullerenes.[1]

In inorganic metal carbide solids, the C_2 units can attain a formal charge of −2 in binary metal carbides (e.g., Li_2C_2, CaC_2, and $M_2(C_2)_3$ with M = Al, La, Pr, or Tb), of −4 in ternary metal carbides containing Ln (lanthanide) metals (e.g., $Ln_3M(C_2)_2$ with M = Fe, Co, Ni, Ru, Os, or Ir), or even of −6 in β-$ScCrC_2$.[23] Hence, the C_2^{3-} species found in $Sc_3C_2@C_{80}$ is unusual. It is the covalent Sc−C_2 dative bond as well as the carbon cage that facilitate the formation of such unusual C_2^{3-} moiety.

At this stage, we would like to further comment on the dynamic behavior of the encased Sc_3C_2 implied by room-temperature ESR[11,12] and NMR[10] experiments on $Sc_3C_2@C_{80}$. As depicted in Figure 1, the three Sc atoms in either the trifoliate $[Sc_3C_2]^{6+}$ cluster of isomer **1a** or the planar $[Sc_3C_2]^{6+}$ cluster of isomer **2a** are not equivalent at all, whereas the C_{80} cage does not maintain the ideal I_h symmetry due to inclusion of the low-symmetric $[Sc_3C_2]^{6+}$ cluster. However, ESR experiments[11,12] suggested that the three Sc atoms of this endofullerene should be equivalent at room temperature, whereas its C_{80} cage is I_h symmetric by displaying only two ^{13}C NMR lines.[10] These phenomena can be understood by taking into account the intramolecular dynamics pertaining to this endofullerene, i.e., rotation of the encased $[Sc_3C_2]^{6+}$ cluster. Tentatively, we have considered the rotation of the $[Sc_3C_2]^{6+}$ cluster around the S_5 axis of the C_{80} (I_h) cage for both isomers **1a** and **2a** by pointwise exploration of the potential energy surface at the GGA-BLYP/DNP theoretical level. As shown in Figures 6 and 7, the estimated activation barriers for the rotations of the trifoliate and planar $[Sc_3C_2]^{6+}$ clusters within isomers **1a** and **2a** are ~4.6 and 1.4 kcal/mol, respectively. The small barriers corroborate that the intramolecular rotation readily occurs at room temper-

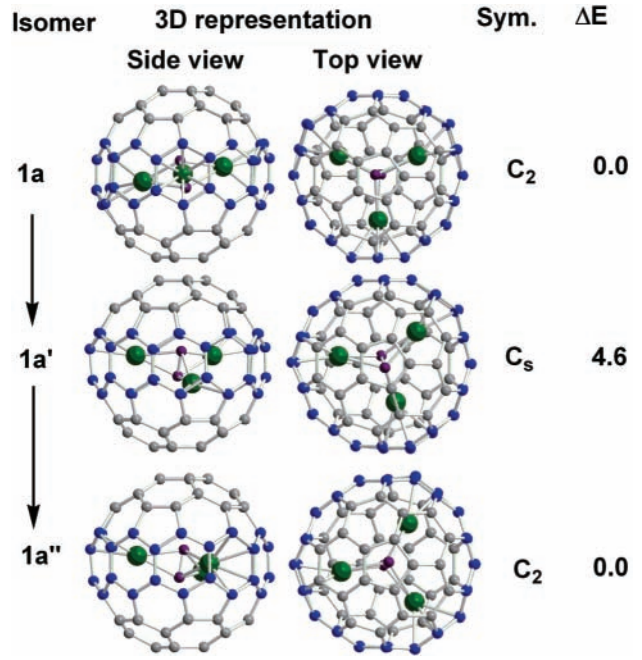

Figure 6. Selected points along the hypothetic route for the top-like spinning of the trifoliate $[Sc_3C_2]^{6+}$ cluster around the S_5 axis of the C_{80} (I_h) cage (BLYP/DNP calculations). The energies (ΔE) are relative to $Sc_3C_2@C_{80}$ isomer **1a. 1a** and **1a″** are equivalent isomers. The rotation proceeds with the Sc atoms rolling round the equatorial cyclacene-like belt (the blue-colored part).

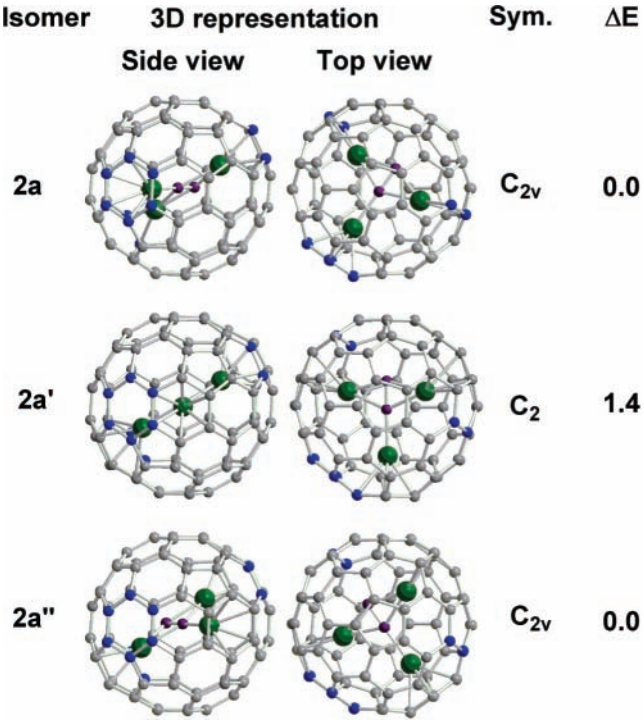

Figure 7. Selected points along the hypothetic route for the rotation of the planar $[Sc_3C_2]^{6+}$ cluster around the S_5 axis of the C_{80} (I_h) cage (BLYP/DNP calculations). The energies (ΔE) are relative to $Sc_3C_2@C_{80}$ isomer **2a. 2a** and **2a″** are equivalent isomers. The carbon atoms of the C_{80} cage that are directly connected to the Sc atoms in isomer **2a** are blue colored.

ature. As such, by averaging over all possible static structures in a long time scale, the three Sc atoms appears to be equivalent, and the C_{80}^{6-} cage appears to be I_h symmetric.[10] Similar intramolecular dynamic behavior was disclosed by ESR experiments on the radical monoanion of $Sc_3N@C_{80}$.[27] On account of such fascinating intramolecular dynamic behavior, quantum mechanical (QM) simulation of the ESR spectrum (e.g., computations of the g-factor and hyperfine coupling constants) by using the static $Sc_3C_2@C_{80}$ geometries is meaningless. To reproduce the experimental ESR data, a QM-based molecular dynamics simulation is essential but unfortunately unapproachable at present.

TABLE 1: GGA-BLYP/DNP-Predicted Relative Energy (ΔE, in eV), C−C Bond Length (R_{CC}, in Å), and Charge State (Q_{CC}) of the C_2 Moiety for the Monocations and Monoanions Derived from $Sc_3C_2@C_{80}$ Isomers 1a and 2a[a]

	1a$^+$	**1a**	**1a**$^-$	**2a**$^+$	**2a**	**2a**$^-$
ΔE	6.31	0.0	−3.33	6.65	0.0	−3.48
R_{CC}	1.27	1.31	1.35	1.27	1.29	1.33
Q_{CC}	−2	−3	−4	−2	−3	−4

[a] For comparison, the computed data for the neutral ones are also given.

3.2. Monocations and Monoanions Derived from $Sc_3C_2@C_{80}$ Isomers 1a and 2a. The optimized geometries of the monocations and monoanions derived from the most stable isomers **1a** and **2a** differ slightly from the neutral ones; the key geometric parameters of them are given in Figures 2 and 3. Their energies relative to the neutral ones are listed in Table 1. The optimal C−C bond length in the encaged Sc_3C_2 cluster is shorten to 1.27 Å for either **1a**$^+$ or **2a**$^+$, indicating the C_2 moiety in either monocation is divalent (C_2^{2-}). Meanwhile, due to absence of π^* electron in C_2^{2-} group (cf., Figures 4a and 5a), the interaction of Sc^{3+} cations with the C_2^{2-} group is primarily ionic; as a result, the Sc−C_2 distances in either **1a**$^+$ or **2a**$^+$ are slightly longer than those in the neutral ones. On the contrary, the C−C bond length is elongated from 1.31 to 1.35 Å for **1a**$^-$, and from 1.29 to 1.33 Å for **2a**$^-$, showing the presence of a C_2^{4-} moiety in either monoanion. The dative bond between the doubly occupied π^* orbital of the central C_2^{4-} group and the d_π orbirals of the surrounding Sc^{3+} cations (cf., Figures 4a and 5a) is stronger than that in the neutral ones, leading to slightly shorter Sc−C_2 bond lengths in the monoanions.

Despite the fact that the neutral **1a** and **2a** are equal in energy, **1a**$^+$ is by 0.34 eV favored over **2a**$^+$, whereas **2a**$^-$ is slightly lower in energy than **1a**$^-$. Hence the monocation and monoanion of $Sc_3C_2@C_{80}$ should adopt the **1a**$^+$ and **2a**$^-$ structures, respectively. Accordingly, the ionization potential and electron affinity predicted for $Sc_3C_2@C_{80}$ at the GGA-BLYP/DNP level are 6.31 and 3.48 eV, respectively. The high electron affinity implies that this endofullerene can be readily reduced to its monoanion form. Indeed, Iiduka et al. found that chemical reduction of this endofullerene to its monoanion can be readily attained with use of n-$Bu_4N^+ClO_4^-$ in pyridine.[10] Earlier electrochemical CV experiments[13] also revealed that the first reduction potential of this endofullerene is only −0.50 V vs ferrocene/ferrocenium (Fc/Fc^+). We shall discuss in detail the redox properties of this endofullerene in the next subsection.

3.3. Electrochemical Redox Properties of $Sc_3C_2@C_{80}$. As shown in Figures 4a and 5a, both neutral $Sc_3C_2@C_{80}$ isomers **1a** and **2a** have a SOMO that is attributed to the covalent dative bonding between the d_π atomic orbitals of Sc^{3+} atoms and the π^* orbital of the C_2 group. However, their lowest unoccupied molecular orbitals (LUMOs) differ significantly in character. The LUMO of isomer **1a** (Figure 4b), quite similar to its SOMO, is localized within the encased trifoliate $[Sc_3C_2]^{6+}$ cluster and can be definitely ascribed to the covalent $d_\pi-\pi^*$ dative bonding between the Sc^{3+} cations and the C_2^{3-} moiety. On the contrary, the LUMO of isomer **2a** is delocalized over the entire molecule with significant contribution from the orbitals of the C_{80} cage.

TABLE 2: Computed Relative Energies (ΔE), the HOMO Energies (E_{HOMO}), and LUMO Energies (E_{LUMO}) of 1a^q and 2a^q (q = +1, 0, −1, −2, −3) in ODCB Solvent, the C−C Bond Length (R_{CC}), and Derived Charge State (Q_{CC}) of the Encased C_2 Moiety, Computed and Experimental[a] Redox Potentials (E^0) of $Sc_3C_2@C_{80}$

	1a$^+$	**2a**$^+$	**1a**	**2a**	**1a**$^-$	**2a**$^-$	**1a**$^{2-}$	**2a**$^{2-}$	**1a**$^{3-}$	**2a**$^{3-}$
Q	1	1	0	0	−1	−1	−2	−2	−3	−3
ΔE (eV)	+5.29	+5.56	+0.02	0.00	−4.29	−4.60	−7.72	−7.60	−10.44	−9.83
E_{HOMO} (eV)[b]	−6.12	−6.05	−4.87	−5.18	−3.88	−4.12	−3.15	−2.53	−2.41	−1.78
E_{LUMO} (eV)[c]	−5.42	−5.63	−4.51	−4.82	−3.42	−3.17	−2.67	−2.37	−1.39	−1.45
R_{CC} (Å)	1.27	1.27	1.31	1.29	1.35	1.33	1.46	1.33	1.69	1.34
Q_{CC}	−2	−2	−3	−3	−4	−4	−5	−4	−6	−4
E^0 (V)	+0.31 (−0.06)[a]					−0.38 (−0.50)[a]	−1.87 (−1.64)[a]		−2.26 (−1.82)[a]	

[a] The experimental redox potentials extracted from ref 13b are given in parentheses. [b] HOMO refers to the highest occupied α-spin−orbital for an open-shell system. [c] LUMO refers to the lowest unoccupied β-spin−orbital for an open-shell system.

Accordingly, when reduced to dianion or trianion, the additional electrons will go solely into the Sc_3C_2 cluster for **1a** but partially into the C_{80} cage for **2a**. Given the bonding character of the LUMO in **1a** and the limited electron-capacity of a highly charged C_{80}^{6-} cage, the dianion and trianion would probably prefer a **1a**-like structure. Thus $Sc_3C_2@C_{80}$ should probably show three reversible reduction states with the charge state ranging from $(Sc^{3+})_3(C_2)^{4-}@C_{80}^{6-}$ to $(Sc^{3+})_3(C_2)^{6-}@C_{80}^{6-}$. Such an inference is consistent with the recently observed electrochemical redox properties of Sc_3C_{82}, i.e., three reversible reductions with potentials at −0.50, −1.64, and −1.82 V vs Fc/Fc^+, and a reversible oxidation with a potential at −0.06 V vs Fc/Fc^+ in 1,2-dichlorobenzene (ODCB) solvent.

To derive theoretically the redox properties of $Sc_3C_2@C_{80}$, we performed GGA-BLYP/DNP calculations on the $[Sc_3C_2@C_{80}]^q$ (q = +1, 0, −1,−2,−3) molecular systems in ODCB solvent. The conductor-like screening model (COSMO)[28] was employed to describe solvent effects. The dielectric constant used in the COSMO calculations is 10.12 for ODCB solvent. For a given redox reaction, reduced form (solvent) → oxidized form (solvent) + e, the computed redox potential E^0 is defined by the equation

$$E^0 = \Delta G - 4.98$$

in which ΔG is the free energy change of the reaction, −4.98 (unit = eV) is the free energy change associated with the reference Fc/Fc^+ reaction (i.e., ferrocenium + e → ferrocene).[29] The three reduction potentials and the first oxidation potential of $Sc_3C_2@C_{80}$ in ODCB can thus be derived on the basis of the predicted total energies of the $[Sc_3C_2@C_{80}]^q$ (q = +1, 0, −1, −2, −3) molecular systems in ODCB solvent.

The computed relative energies of isomers **1a**^{q} and **2a**^{q} (q = +1, 0, −1, −2, −3) in ODCB solvent are listed in Table 2, along with the C−C bond length and derived charge state of the carbide C_2 moiety. On the basis of the computed relative energies, the preferential reduction states of $Sc_3C_2@C_{80}$ in ODCB solvent are **2a**$^-$, **1a**$^{2-}$, and **1a**$^{3-}$, whereas its favorable oxidation state is **1a**$^+$. Thus the geometry of the encased Sc_3C_2 cluster is highly sensitive to the charge state of the whole molecule, adopting a planar structure in the neutral molecule and monoanion and shifting to trifoliate structures in the monocation, dianion and trianion. On the basis of the relative energies of these redox states, the electrochemical redox potentials of $Sc_3C_2@C_{80}$ in ODCB were computed and given in Table 2. The agreement of the theoretical data with the experimental ones is fairly good, except that the third reduction potential is overestimated by 0.36 V.

It is noteworthy that the three reduction states of this endofullerene, i.e., $[Sc_3C_2@C_{80}]^q$ (q = −1, −2, −3), have the electronic states $(Sc^{3+})_3C_2^{(3-q)-}@C_{80}^{6-}$ with the C−C bond length of the encased C_2 moiety being elongated from 1.33 to 1.69 Å (cf. Table 2). In particular, the trianion $[Sc_3C_2@C_{80}]^{3-}$ has a rather compact trifoliate $[Sc_3C_2]^{3+}$ cluster with a rather short $Sc<C_{carbide}$ bond of ∼2.06 Å and a long C−C bond of 1.69 Å for the carbide moiety. Accordingly, the carbide moiety in this reduction state can be well described as μ_3-η_2-C_2^{6-}. So far such a peculiar carbide moiety can only be found in the β-$ScCrC_2$ solid, which contains analogous trifoliate $[Cr_3C_2]^{3+}$ clusters.[23]

4. Concluding Remarks

In summary, we have shown by means of DFT calculations that the open-shell metal−carbide endofullerene $Sc_3C_2@C_{80}$ has the charge state $(Sc^{3+})_3(C_2)^{3-}@C_{80}^{6-}$. The presence of a lot of low-lying isomers differing in geometries and locations of the endohedral $[(Sc^{3+})_3(C_2)^{3-}]$ cluster implies unusual dual intramolecular dynamic behaviors pertaining to this endofullerene at room temperature, i.e., nearly free rotation of the endohedral cluster within the I_h-symmetric C_{80}^{6-} as well as dynamic geometric fluctuation of the endohedral cluster between a planar structure and a trifoliate structure.

The electrochemical redox properties of this endofullerene observed experimentally have been reproduced and elucidated in terms of electronic structure theory. The redox states of this endofullerene, including three reversible reduction states and one reversible oxidation state, follow the general charge-state formula $(Sc^{3+})_3C_2^{(3-q)-}@C_{80}^{6-}$ (q is the charge of the whole molecule) and differ solely in the charge state of the central C_2 carbide moiety that varies sequentially from C_2^{2-} (for q = +1) to C_2^{6-} (for q = −3). This demonstrates the high charge flexibility of the endohedral metal−carbide cluster arising from the flexible charge states of the central C_2 carbide moiety.[23] More interestingly, the structure of the endohedral $[(Sc^{3+})_3C_2^{(3-q)-}]$ cluster appears to be highly sensitive to the charge state of the whole molecule, varying from the planar structure (for q = 0 and −1) to the trifoliate structure (for q = +1, −2, −3).

Finally, we should emphasize that the high charge-flexibility of endohedral metal−carbide cluster disclosed herein should play an important role in the chemistry of endohedral metallofullerenes. For example, since $Sc_3C_2@C_{80}$ has an endohedral $(Sc^{3+})_3C_2^{3-}$ cluster, further addition of a Sc atom into this endofullerene would lead to the formation of $Sc_4C_2@C_{80}$ that likely has the charge state $(Sc^{3+})_4C_2^{6-}@C_{80}^{6-}$. Note that this new endofullerene containing an unprecedentedly large six-membered metal carbide cluster is in a stoichiometry of Sc_4C_{80}. It should be mentioned that isolation of Sc_4C_{82} was once claimed without structural characterization by Shinohara group.[1,30] We believe the $Sc_4C_2@C_{80}$ structure could be a rational structural model for the previously synthesized tetrametallofullerene Sc_4C_{82}.[31]

Acknowledgment. This work was supported by NSFC (Grants No. 20021002, 20425312, 20203013, 20423002).

Supporting Information Available: Cartesian coordinates for the GGA-BLYP/DNP-optimized geometries of $Sc_3C_2@C_{80}$ isomers, their relative energies predicted at the GGA-P91/DNP level theory, as well as the Cartesian coordinates and total energies of $[Sc_3C_2@C_{80}]^q$ ($q = +1, 0, -1, -2, -3$) in ODCB solvent predicted by GGA-BLYP/DNP COSMO calculations. This material is available free of charge via the Internet at http://pubs.acs.org.

References and Notes

(1) Shinohara, H. *Rep. Prog. Phys.* **2000**, *63*, 843.

(2) (a) Wang, C.-R.; Kai, T.; Tomiyama, T.; Yoshida, T.; Kobayashi, Y.; Nishibori, E.; Takata, M.; Sakata, M.; Shinohara, H. *Nature* **2000**, *408*, 426. (b) Takata, M.; Nishibori, E.; Wang, C. R.; Sakata, M.; Shinohara, H. *Chem. Phys. Lett.* **2003**, *372*, 512. (c) Kobayashi, K.; Nagase, S. *Chem. Phys. Lett.* **2003**, *362*, 373.

(3) (a) Stevenson, S.; Fowler, P. W.; Heine, T.; Duchamp, J. C.; Rice, G.; Glass, T.; Harich, K.; Hajdu, E.; Bible, R.; Dorn, H. C. *Nature* **2000**, *408*, 428. (b) Olmstead, M. M.; Lee, H. M.; Duchamp, J. C.; Stevenson, S.; Marciu, D.; Dorn, H. C.; Balch, A. L. *Angew. Chem., Int. Ed.* **2003**, *42*, 900.

(4) Kato, H.; Taninaka, A.; Sugai, T.; Shinohara, H. *J. Am. Chem. Soc*. **2003**, *125*, 7782.

(5) Kroto, H. W. *Nature*, **1987**, *329*, 529.

(6) Shimotani, H.; Ito, T.; Iwasa, Y.; Taninaka, A.; Shinohara, H.; Nishibori, E.; Takata, M.; Sakata, M. *J. Am. Chem. Soc.* **2004**, *126*, 364 and references therein.

(7) (a) Stevenson, S.; Rice, G.; Glass, T.; Harich, K.; Croner, F.; Jordan, M. R.; Craft, J.; Hadju, E.; Bible, R.; Olmstead, M. M.; Maitra, K.; Fisher, A. J.; Balch, A. L.; Dorn, H. C. *Nature* **1999**, *401*, 55. (b) Olmstead, M. M.; de Bettencourt-Dias, A.; Duchamp, J. C.; Stevenson, S.; Marciu, D.; Dorn, H. C.; Balch, A. L. *Angew. Chem., Int. Ed.* **2001**, *40*, 1223.

(8) (a) Wang, C. R.; Kai, T.; Tomiyama, T.; Yoshida, T.; Kobayashi, Y.; Nishibori, E.; Takata, M.; Sakata, M.; Shinohara, H. *Angew. Chem., Int. Ed.* **2001**, *40*, 397. (b) Krause, M.; Hulman, M.; Kuzmany, H.; Dubay, O.; Kresse, G.; Seifert, G.; Wang, C.; Shinohara, H. *Phys. Rev. Lett*. **2004**, *93*, 137403.

(9) (a) Tan, K.; Lu, X. *Chem. Commun.* **2005**, 4444. (b) Cao, B.; Hasegawa, M.; Okada, K.; Tomiyama, T.; Okazaki, T.;. Suenaga, K.; Shinohara, H. *J. Am. Chem. Soc.* **2001**, *123*, 9679. (c) Yumura, T.; Sato, Y.; Suenaga, K.; Iijima, S. *J. Phys. Chem. B* **2005**, *109*, 20251.

(10) Iiduka, Y.; Wakahara, T.; Nakahodo, T.; Tsuchiya, T.; Sakuraba, A.; Maeda, Y.; Akasaka, T.; Yoza, K.; Horn, E.; Kato, T.; Liu, M. T. H.; Mizorogi, N.; Kobayashi, K.; Nagase, T. *J. Am. Chem. Soc*. **2005**, *127*, 12500. Note that the X-ray diffraction data indicated a planar Sc_3C_2 structure in the monoadduct of $Sc_3C_2@C_{80}$ functionalized by adamantylide carbene, whereas preliminary DFT calculations predicted the endohedral cluster in neutral $Sc_3C_2@C_{80}$ can be either planar or trifoliate.

(11) (a) Shinohara, H.; Sato, H.; Ohkohchi, M.; Ando, Y.; Kodama, T.; Shida, T.; Kato, T.; Saito, Y. *Nature* **1992**, *357*, 52. (b) Yannoni, C. S.; Hoinkis, M.; Vries, M. S. D.; Bethune, D. S.; Salem, I. R.; Crowder, M. S.; Johnson, R. D. *Science* **1992**, *256*, 1191.

(12) (a) Shinohara, H.; Inakuma, M.; Hayashi, N.; Sato, H.; Saito, Y.; Kato, T.; Bandow, S. *J. Phys. Chem*. **1994**, *98*, 8597−8599. (b) van Loosdrecht, P. H. M.; Johnson, R. D.; de Vries, M. S.; Kiang, C. H.; Bethune, D. S.; Dorn, H. C.; Burbank, P.; Stevenson, S. *Phys. Rev. Lett*. **1994**, *73*, 3415−3418. (c) Kato, T.; Bandow, S.; Inakuma, M.; Shinohara, H. *J. Phys. Chem.* **1995**, *99*, 856. (d) Bartl, A.; Dunsch, L. *Synth. Metals* **2001**, *121*, 1147−1148. (e) Kato, T.; Okubo, S.; Inakuma, M.; Shinohara, H. *Phys. Solid State* **2002**, *44*, 398−400.

(13) (a) Anderson, M. R.; Dorn, H. C.; Stevenson, S.; Burbank, P. M.; Gibson, J. R. *J. Am. Chem. Soc*. **1997**, *119*, 437. (b) Wakahara, T.; Sakuraba, A.; Iiduka, Y.; Okamura, M.; Tsuchiya, T.; Maeda, Y.; Akasaka, T.; Okubo, S.; Kato, T.; Kobayashi, K.; Nagase, S.; Kadish, K. M. *Chem. Phys. Lett.* **2004**, *398*, 553.

(14) Takata, M.; Nishibori, E.; Sakata, M.; Inakuma, M.; Yamamoto, E.; Shinohara, H. *Phys. Rev. Lett.* **1999,** *83*, 2214.

(15) (a) Ungerer, J. R.; Hughbanks, T. *J. Am. Chem. Soc.* **1993**, *115*, 2054. (b) Kobayashi, K.; Nagase, S. *Chem. Phys. Lett.* **1999**, *313*, 45.

(16) Fowler, P. W.; Manolopoulos, D. E. *An Atlas of Fullerenes*; Clarendon Press: Oxford, 1995.

(17) (a) Becke, A. D. *J. Chem. Phys.* **1988**, *88*, 2547. (b) Lee, C.; Yang, W.; Parr, R. G. *Phys. Rev. B* **1988**, *37*, 786.

(18) (a) Delley, B. *J. Chem. Phys.* **1990**, *92*, 508. (b) Delley, B. *J. Chem. Phys.* **2000**, *113*, 7756. $DMol^3$ is available as part of Material Studio and Cerius2 by Accelrys Inc.

(19) Perdew, J. P. In *Electronic Structure of Solids '91*; Ziesche, P., Eschrig, H., Eds.; Akademie Verlag: Berlin, 1991; p 11.

(20) (a) Handy, N. C.; Knowles, P. J.; Somasundram, K. *Theor. Chim. Acta* **1985**, *68*, 87. (b) Nobes, R. H.; Pople, J. A.; Radom, L.; Handy, N. C.; Knowles, P. J. *Chem. Phys. Lett.* **1987**, *138*, 481

(21) (a) Baker, J.; Scheiner, A.; Andzelm, J. *Chem. Phys. Lett.* **1993**, *216*, 380. (b) Johnson, B. G.; Gonzalez, C. A.; Gill, P. M. W.; Pople, J. A. *Chem. Phys. Lett.* **1994**, *221*, 100.

(22) Emsley, J. *The Elements*; Clarendon: Oxford, U.K., 1989; p 174.

(23) (a) King, R. B. *J. Organomet. Chem.* **1997**, *536/537*, 7. (b) Cotton, F. A.; Wilkinson, G. C.; Murillo, A.; Bochmann, M. *Advanced Inorganic Chemistry*, 6th ed.; Wiley-Interscience: New York, 1999; p 221.

(24) Sc^{2+} was long supposed for Sc_2C_{84}, but recent experiments showed it is more likely Sc^{3+}. See: Pichler, T.; Hu, Z.; Grazioli, C.; Legner, S.; Knupfer, M.; Golden, M. S.; Fink, J.; de Groot, F. M. F.; Hunt, M. R. C.; Rudolf, P.; Follath, R.; Jung, C.; Kjeldgaard, L.; Bruhwiler, P.; Inakuma, M.; Shinohara, H. *Phys. Rev. B* **2000**, *62*, 13196 and references therein.

(25) Sc^{2+} was supposed for $Sc@C_{82}$, but recent DFT computations clearly showed it is Sc^{3+}. See: Lu, J.; Zhang, X. W.; Zhao, X. G.; Nagase, S.; Kobayashi, K. *Chem. Phys. Lett.* **2000**, *332*, 219 and references therein.

(26) Campanera, J. M.; Bo, C.; Olmstead, M. M.; Balch, A. L.; Poblet, J. M. *J. Phys. Chem. A* **2002**, *106*, 12356.

(27) Jakes P.; Dinse, K.-P. *J. Am. Chem. Soc*. **2001**, *123*, 8854.

(28) *28. (a) Klamt, A.; Schüürmann, G. J. Chem. Soc., Perkin Trans. 2* **1993**, 799. (b) Klamt A., Jonas V., Burger T., Lohrenz J. *J. Phys. Chem.* **1998**, *102*, 5074.

(29) Ryan, M. F.; Eyler, J. R.; Richardson, D. E. *J. Am. Chem. Soc*. **1992**, *114*, 8611.

(30) Wang, C. R.; Inakuma, M.; Shinohara, H. *Chem. Phys. Lett.* **1999**, *300*, 379.

(31) Tan, K.; Lu, X.; Wang, C.-R. Unpublished results.